ISSN 1674-1056
http://cpb.iphy.ac.cn
http://iopscience.iop.org/cpb
中国物理 B
Chinese Physics
中国物理 Chinese Physics B

Electronic states and molecular orientation of ITIC film

Ying-Ying Du(杜莹莹), De-Qu Lin(林德渠), Guang-Hua Chen(陈光华), Xin-Yuan Bai(白新源), Long-Xi Wang(汪隆喜), Rui Wu(吴蕊), Jia-Ou Wang(王嘉鸥), Hai-Jie Qian(钱海杰), Hong-Nian Li(李宏年)
Citation: Chin. Phys. B . 2018, 27(8): 088801. **doi:** 10.1088/1674-1056/27/8/088801

Journal homepage: http://cpb.iphy.ac.cn; http://iopscience.iop.org/cpb

What follows is a list of articles you may be interested in

Self-assembled monolayer modified copper(I) iodide hole transport layer for efficient polymer solar cells

Yuancong Zhong(钟远聪), Qilun Zhang(张琪伦), You Wei(魏优), Qi Li(李琦), Yong Zhang(章勇)
Chin. Phys. B . 2018, 27(7): 078802. **doi:** 10.1088/1674-1056/27/7/078802

Efficient ternary organic solar cells with high absorption coefficient DIB-SQ as the third component

Hui-Xin Qi(齐慧欣), Bo-Han Yu(余泊含), Sai Liu(刘赛), Miao Zhang(张苗), Xiao-Ling Ma(马晓玲), Jian Wang(王健), Fu-Jun Zhang(张福俊)
Chin. Phys. B . 2018, 27(5): 058802. **doi:** 10.1088/1674-1056/27/5/058802

A simulation study on p-doping level of polymer host material in P3HT: PCBM bulk heterojunction solar cells

Hossein Movla, Mohammad Babazadeh
Chin. Phys. B . 2017, 26(4): 048802. **doi:** 10.1088/1674-1056/26/4/048802

Sodium chloride methanol solution spin-coating process for bulk-heterojunction polymer solar cells

Tong-Fang Liu(刘统方), Yu-Feng Hu(胡煜峰), Zhen-Bo Deng(邓振波), Xiong Li(李熊), Li-Jie Zhu(朱丽杰), Yue Wang(王越), Long-Feng Lv(吕龙锋), Tie-Ning Wang(王铁宁), Zhi-Dong Lou(娄志东), Yan-Bing Hou(侯延冰), Feng Teng(滕枫)
Chin. Phys. B . 2016, 25(8): 088801. **doi:** 10.1088/1674-1056/25/8/088801

Effects of acetone-soaking treatment on the performance of polymer solar cells based on P3HT/PCBM bulk heterojunction

Liu Yu-Xuan, Lü Long-Feng, Ning Yu, Lu Yun-Zhang, Lu Qi-Peng, Zhang Chun-Mei, Fang Yi, Tang Ai-Wei, Hu Yu-Feng, Lou Zhi-Dong, Teng Feng, Hou Yan-Bing
Chin. Phys. B . 2014, 23(11): 118802. **doi:** 10.1088/1674-1056/23/11/118802

Electronic states and molecular orientation of ITIC film*

Ying-Ying Du(杜莹莹)[1], De-Qu Lin(林德渠)[1], Guang-Hua Chen(陈光华)[1], Xin-Yuan Bai(白新源)[1], Long-Xi Wang(汪隆喜)[1], Rui Wu(吴蕊)[2], Jia-Ou Wang(王嘉鸥)[2], Hai-Jie Qian(钱海杰)[2], and Hong-Nian Li(李宏年)[1,†]

[1] *Department of Physics, Zhejiang University, Hangzhou* 310027, *China*
[2] *Institute of High Energy Physics, Chinese Academy of Sciences, Beijing* 100049, *China*

(Received 18 April 2018; revised manuscript received 7 May 2018; published online 10 July 2018)

ITIC is the milestone of non-fullerene small molecule acceptors used in organic solar cells. We study the electronic states and molecular orientation of ITIC film using photoelectron spectroscopy and x-ray absorption spectroscopy. The negative integer charge transfer energy level is determined to be 4.00 ± 0.05 eV below the vacuum level, and the ionization potential is 5.75 ± 0.10 eV. The molecules predominantly have the face-on orientation on inert substrates as long as the surfaces of the substrates are not too rough. These results provide the physical understanding of the high performance of ITIC-based solar cells, which also afford implications to design more advanced photovoltaic small molecules.

Keywords: electronic states, molecular orientation, photovoltaic small molecule, photoelectron spectroscopy, XAS

PACS: 88.40.jr, 73.30.+y, 61.46.–w, 61.05.cj **DOI:** 10.1088/1674-1056/27/8/088801

1. Introduction

Organic solar cells (OSCs) have attracted extensive attention during the past two decades due to the advantages of light weight, mechanical flexibility, low cost, and large-scale solution-fabrication. This type of solar cell comprises a thin layer of electron donor/electron acceptor blend sandwiched between two electrodes. Fullerene derivatives such as $PC_{61}BM$[1] and $PC_{71}BM$[2] have been the most popular electron acceptors. However, fullerene derivatives have the drawback of very weak photo-absorption in the visible and near-infrared regions. Therefore, a high-performance non-fullerene acceptor is highly desirable. Very recently a few non-fullerene acceptors have been developed, which exhibited a comparable photovoltaic property with $PC_{61}BM$ or $PC_{71}BM$. Among them, 3,9-bis(2-methylene-(3-(1,1-dicyanomethylene)-indanone)-5,5,11,11-tetrakis(4-hexylphenyl)-dithieno[2,3-d:2′,3′-d′]-s-indaceno[1,2-b:5,6-b′]-dithiophene (ITIC) is the milestone molecule.[3] The OSC based on ITIC exhibited a power conversion efficiency of 11.21%,[4] and the existing more advanced non-fullerene acceptors are the modification of ITIC.[5–11]

The energy position of the highest occupied molecular orbital (HOMO) and the lowest unoccupied molecular orbital (LUMO) play crucial roles in the performance of OSCs. The HOMO level, or the top of the HOMO band (E_{HOMO} (top)) for solid samples, is the minus of ionization potential (IP) if referenced to the vacuum level. The IP of ITIC was measured to be 5.48 eV–5.67 eV with the cyclic voltammetry method for solution samples.[4,11–16] Considering the fact that ITIC behaves as a solid state in OSCs, the IP of a film sample is desirable. One purpose of this work is to obtain the IP of ITIC film with ultraviolet photoelectron spectroscopy (UPS) measurements.

For electron acceptor materials such as ITIC, the LUMO level is more pertinent to the performance of OSCs as compared with the HOMO level. The energy position of the bottom of the LUMO band (E_{LUMO} (bottom)) is the negative electron affinity (EA). The EA was measured to be 3.63 eV–4.00 eV with the cyclic voltammetry method for solution samples.[4,11–16] The result for a film sample has not been reported in the literature. Actually, the concept of the LUMO level (or E_{LUMO} (bottom)) should be replaced by the concept of the negative integer charge transfer level ($E_{\mathrm{ict-}}$) in many aspects of the performance of OSCs.[17] The energy position of $E_{\mathrm{ict-}}$ is slightly lower than that of the E_{LUMO} (bottom), i.e., the absolute value of $E_{\mathrm{ict-}}$ is slightly greater than that of EA. More details about the concept of $E_{\mathrm{ict-}}$ can be found in Refs. [18]–[21] and will be narrated later. $E_{\mathrm{ict-}}$ can be measured with UPS, and the measured $E_{\mathrm{ict-}}$ has been reported for many organic molecules.[17,19,22,23] Although there are a few UPS data of ITIC film in Refs. [7] and [16], the $E_{\mathrm{ict-}}$ has not been determined. The main purpose of our work is to measure the $E_{\mathrm{ict-}}$ of ITIC film.

Molecular orientation has a significant effect on charge transport. For planar organic molecules, face-on (with the molecular plane parallel to the substrate) and edge-on (with the molecular plane perpendicular to the substrate) are two frequently encountered orientations. The face-on orientation is more beneficial to the charge transport in OSCs, since the

*Project supported by the National Natural Science Foundation of China (Grant Nos. 11374258 and 11079028).
†Corresponding author. E-mail: phylihn@mail.zju.edu.cn
© 2018 Chinese Physical Society and IOP Publishing Ltd

stacking of the π (and π^*) orbital forms the charge transport channel across the device.[24–26] The molecular orientation in ITIC film was found to be substrate-dependent according to some grazing incidence wide-angle x-ray scattering (GIWXAS) measurements.[13,14,27,28] To obtain an in-depth understanding of the molecular orientation, we prepare the ITIC film samples on some different inert substrates and perform x-ray absorption spectroscopy (XAS) measurements. The XAS data also provide some information about the unoccupied electronic states.

2. Experiment

We utilized three substrates, naturally oxidized Al (111) single crystal, ITO glass, and Si:H (111), to study the electronic states and the molecular orientation. The Al (111) single crystal was simply cleaned by sonication in de-ionized water and acetone. The ITO glass was ultrasonically cleaned with detergent for 30 min, washed with much de-ionized water, and further ultrasonically cleaned with de-ionized water, acetone, and isopropyl alcohol. The Si:H (111) substrate was prepared as follows. Si (111) wafers were first ultrasonically cleaned in deionized water and ethyl alcohol. Then the wafers were rinsed sequentially in solution 1 ($NH_3{\cdot}H_2O$:H_2O_2:H_2O = 1:1:6, 80 °C, 15 min) and solution 2 (HCl:H_2O_2:H_2O = 1:1:6, 80 °C, 15 min). After being washed in deionized water, the wafers were etched in 5% HF for 1 min to obtain the H-passivated Si (111) surface. Finally, the Si:H (111) wafers were again rinsed in deionized water for less than 5 s to remove residual compounds from the etching process. After being cleaned, the substrates were dried by nitrogen flow and transferred into a nitrogen-filled glove box immediately. In the following we denote the naturally oxidized Al (111) single crystal, the ITO glass, and the Si:H (111) as Al, ITO, and Si, respectively.

ITIC powder (purity $>$ 99%) was purchased from the Solenne company. The powder was dissolved in chlorobenzene at a concentration of 25 mg/mL. The solution was stirred at 70 °C for $\sim$ 24 h and filtrated through a polytetrafluoroethylene filter (0.2 μm). The ITIC films were then spin coated (2000 rpm for 60 s) on the substrates. After being spin-coated, the samples were annealed on a hot plate at 130 °C for 10 min. All the above experimental operations were carried out in the glove box. The thickness values of the films were not quantitatively calibrated but they were appropriate for our study. The signals of the substrates were totally attenuated, and the charging effect was not observed in the UPS measurements.

The ITIC film samples were placed in a small plastic box in the glove box, and the plastic box was well sealed with parafilm before being fetched out. Spectral measurements were carried out at the Photoelectron Spectroscopy Endstation of the Beijing Synchrotron Radiation Facility (BSRF). The samples were clamped onto stainless steel sample holders in a helium-filled glove box of BSRF and then transported into the vacuum system of the endstation; the time exposure to air was less than 30 s in this process. We measured the spectra more than six hours after the samples had been left in the ultra high vacuum environment (2×10^{-10} mbar, 1 bar = 10^5 Pa). The UPS spectra were measured with a photon energy of 21.2 eV and a VG Scienta R4000 analyzer. The sample normal direction coincided with the entrance of the energy analyzer, and the photoelectrons with different emission angles (within $\pm 19°$ with respect to the sample normal direction) were integrated. In the work function measurement, we applied -5.0 V bias to the sample. The overall energy resolution was better than 0.05 eV. X-ray photoelectron spectra (XPS) were also measured for a portion of the samples with a photon energy of 700 eV; the overall energy resolution was $\sim$ 0.75 eV. Carbon K-edge XAS spectra were acquired with the total electron yield mode; the energy resolution was $\sim$ 0.2 eV. For helping to understand the XAS data we slightly doped the ITIC/Si sample by depositing Ca atoms onto the sample surface. The Ca atoms were evaporated from a Ta boat mounted in the ultra-high vacuum system.

C and O contamination should be well controlled for reliable spectra measured on ex-situ prepared samples. ITIC itself contains both C and O atoms, and the possible contamination cannot be checked by UPS or XPS measurements. So we prepared and measured some $PC_{61}BM$ and P3HT samples (the latter molecule does not contain O atom) to check the contamination. The measured UPS spectrum of the spin coated $PC_{61}BM$ film was unexpectedly the same as that of the $PC_{61}BM$ film prepared by vacuum deposition.[29] The O 1s signal was not observed in the XPS spectrum of the P3HT sample. So the ITIC samples of this work were very clean, and the measured spectra are of high quality.

For helping to understand the experimental data we perform the density functional theory (DFT) calculations for isolated ITIC molecule. The calculating details are the same as those we described previously.[29,30]

3. Results and discussion

Figure 1 shows the optimized structure of ITIC molecule and the energy level diagram near the HOMO and LUMO levels. The main chain where most of the π electrons are located is planar. The energy levels are for ground state, and the HOMO–LUMO gap (1.193 eV) in Fig. 1(b) should be much smaller than the experimentally measured gap. However, the energy intervals between the occupied levels are generally (though not always) reliable.[29–31]

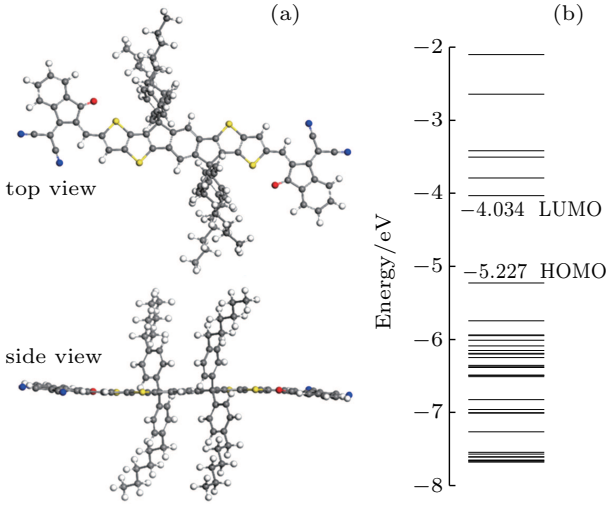


Fig. 1. (color online) (a) Optimized structure of ITIC by DFT calculations. The gray, white, red, blue, and yellow balls represent C, H, O, N, and S atoms, respectively. (b) Energy level diagram near HOMO and LUMO levels.

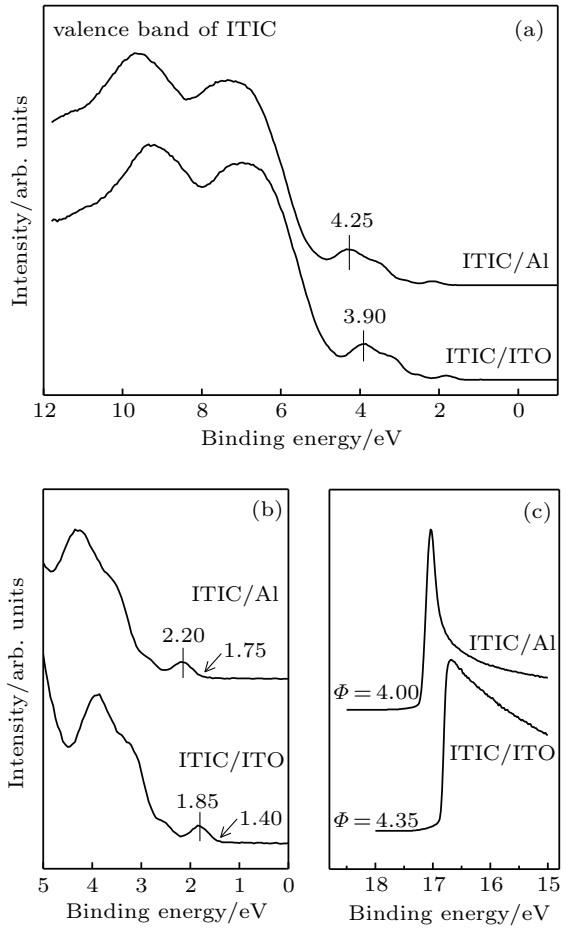


Fig. 2. (a) UPS data of ITIC films on Al and ITO substrates. (b) Enlarged view of photoemission between Fermi level (0 eV) and 5.0-eV binding energy. (c) Secondary electron cutoffs. Work function data indicated in panel (c) are determined by the tangent of cutoff and base line.

Figure 2(a) shows the UPS data of the ITIC/Al and ITIC/ITO samples. The spectra in Fig. 2(a) are normalized to the height of the feature at 4.25 eV in the ITIC/Al spectrum (3.90 eV in the ITIC/ITO spectrum). The reason for the different binding energies of the two spectra will be explained later. Figure 2(b) enlarges the spectral features between the Fermi level and 5-eV binding energy; the spectral shape is much the same as the reported spectrum shapes.[7,16] Comparing Fig. 2(b) with Fig. 1(b), the calculated energy levels correctly predict that the HOMO signal is well separated from the signals of the other occupied levels. The center of the HOMO photoemission is located at 2.20 eV for the ITIC/Al sample and 1.85 eV for the ITIC/ITO sample. We do not show the UPS spectra of the ITIC/Si sample because they cannot provide more information than what can be drawn from Fig. 2.

UPS is a most powerful tool to measure the IP of a solid sample. IP is the energy difference between the E_{HOMO} (top) and the vacuum level. According to Fig. 2(b) the E_{HOMO} (top) is located at ~ 1.75 eV and ~ 1.40 eV for the ITIC/Al and ITIC/ITO sample, respectively. The vacuum level (identical to the work function Φ) is indicated in Fig. 2(c). The value of the IP obtained for the ITIC/Al sample ($1.75 + 4.00 = 5.75$ eV) is the same as that for the ITIC/ITO sample ($1.40 + 4.35 = 5.75$ eV), which is reasonable because IP has little relation to the substrates. The experimental error, including some arbitrariness in determining the energy position of the E_{HOMO} (top) in Fig. 2(b), is at most ± 0.10 eV. The IP of 5.75 ± 0.10 eV for our film samples is somewhat different from that (5.48 eV–5.67 eV)[4,11–16] measured by cyclic voltammetry. Our result is more practical since ITIC behaves as solid state in OSCs.

UPS is also a most powerful tool to measure $E_{\mathrm{ict-}}$. In this case the substrate has to be properly selected. For understanding this we explain the concept of $E_{\mathrm{ict-}}$ in some detail. $E_{\mathrm{ict-}}$ was proposed for the energy level alignment at the interface between an electron acceptor material and an inert substrate.[18–21] This kind of interface is frequently encountered in OSCs fabricated by spin coating. The overlapping of the electronic wave functions is negligible at the interface, but charge transfer across the interface can be realized by the tunneling of integer charge. If the work function of the substrate is sufficiently small, some electrons can transfer from the substrate to the $E_{\mathrm{ict-}}$ of the acceptor material. $E_{\mathrm{ict-}}$ is lower in energy than the E_{LUMO} (bottom) because of two reasons. First, the state accommodating the electrons transferred from the substrate may be the negative polaron (or bi-polaron) state due to the soft nature of many organic molecules.[32] As is well known, the negative polaron level is lower than the E_{LUMO} (bottom). Second, the disordered structure of an organic film can induce the tail state of the LUMO band extending into the HOMO-LUMO gap by several tenths of eV.[20,33,34] The tail state can also accommodate the electrons transferred from the substrate to pin the Fermi level although the density of states (DOS) of the tail state is generally too weak to be detected by conventional UPS measurements.

According to the meaning of $E_{\mathrm{ict}-}$, the substrate for measuring the $E_{\mathrm{ict}-}$ of an organic acceptor material must be inert and have a small work function. The Al (with natural oxide layer) and ITO substrate are both inert. The work function of our Al substrate is 3.45 eV–3.53 eV as measured on several samples (without the ITIC overlayer); the work function of the ITO substrate is 4.30 eV–4.50 eV. In Fig. 2(c) the work function of the ITIC/Al sample (4.00 eV) is greater than that of the substrate, indicating the electrons transfer from the Al substrate to the ITIC film. The Fermi level is then pinned at the $E_{\mathrm{ict}-}$, and the measured work function is identical to the $E_{\mathrm{ict}-}$ (the value of $E_{\mathrm{ict}-}$, by convention, is the absolute value of the energy position of $E_{\mathrm{ict}-}$ relative to the vacuum level). Considering the experimental error, we obtain the conclusion of $E_{\mathrm{ict}-} = 4.00 \pm 0.05$ eV for ITIC. The $E_{\mathrm{ict}-}$ of ITIC is close to that of $PC_{61}BM$ (~ 3.94 eV),[17] which is one of the reasons why ITIC can substitute for fullerene acceptors.

By comparison, the work function of the ITIC/ITO sample is 4.35 eV, close to that of the ITO substrate. This is because the work function of the ITO substrate (4.30 eV–4.50 eV) is greater than $E_{\mathrm{ict}-}$ (4.00 eV). The electron cannot transfer from the ITO substrate to the ITIC film, and the electrons cannot transfer from the ITIC film to the ITO substrate either, since the LUMO level is empty and the HOMO level is much lower than the Fermi level of the substrate (see Fig. 1(b)). The ITIC/ITO interface is thus vacuum level alignment, and the work function of the ITIC/ITO sample should be the same as that of the substrate. Owing to the different schemes of energy level alignment, the valence band features also present different binding energies for the ITIC/Al and ITIC/ITO samples in Figs. 2(a) and 2(b).

The carbon K-edge XAS spectra of ITIC/Al, ITIC/ITO, and ITIC/Si are shown in Fig. 3. The spectral shape, peak position, and angle dependence are very similar for the three samples. The absorption from the C 1s states to the localized π^* or σ^* orbitals is distributed between 284.0 eV and 290.5 eV; distributed above 290.5 eV is the absorption to the continuum states (ionization). According to the $E_{\mathrm{ict}-}$ of 4.00 eV the distribution of the localized π^* and σ^* orbitals should be within an energy range of 4.00 eV. The seeming discrepancy is due to the broad distribution of the C 1s states (the initial states of the photon absorption) as indicated in the inset of Fig. 3(a).

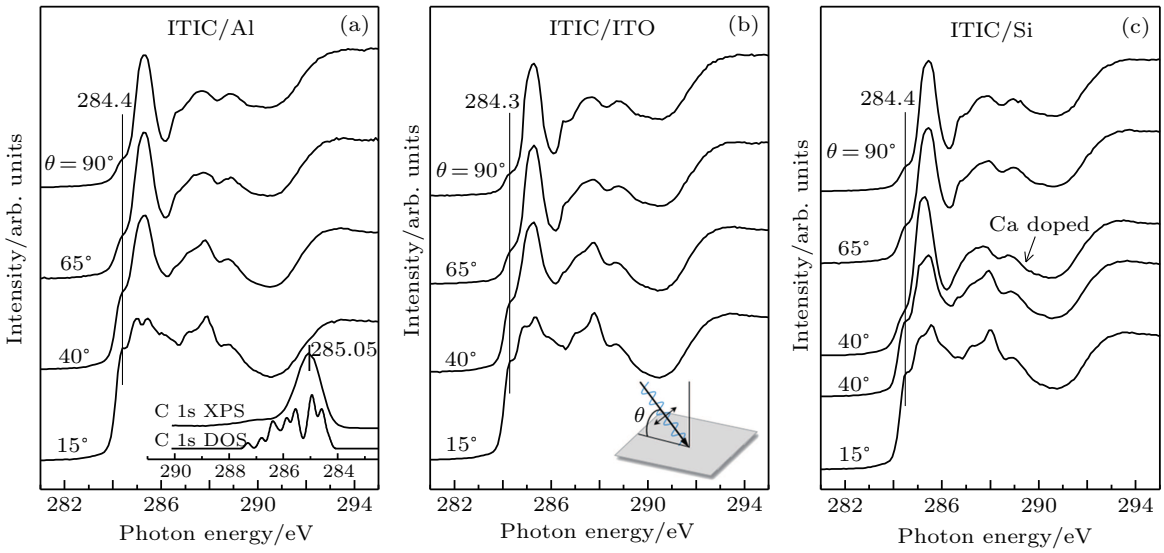


Fig. 3. Angle-dependent C K-edge XAS spectra of ITIC film on (a) Al, (b) ITO, and (c) Si substrate, where the spectra are normalized to the intensity at $h\upsilon = 295$ eV in each panel. In panel (c), the spectrum of the Ca-doped ITIC/Si (indicated by an arrow) is also shown for comparison. The inset in panel (a) shows the C 1s XPS spectrum of the ITIC/Al and the C 1s DOS calculated for the ITIC molecule; the energy of DOS has been shifted to coincide with the binding energy of the XPS spectrum. Inset in panel (b) displays the definition of θ.

The first feature of the XAS spectrum is located at 284.4 eV in Figs. 3(a) and 3(c) (or 284.3 eV in Fig. 3(b), the difference is within the experimental error). The first feature generally corresponds to the absorption to the LUMO (and possibly the adjacent LUMO+1). Considering the broad distribution of the C 1s states, however, the final states of the first feature should be checked for the samples studied here. The spectrum of the Ca-doped ITIC/Si affords the necessary verification. This spectrum is measured at $\theta = 40°$ and is shown next to the 40° spectrum of the un-doped sample in Fig. 3(c). The intensity of the first feature obviously decreases for the doped sample as compared with that of the un-doped sample. We do not perform the doping experiments in detail, and the sample is only slightly doped. Only the LUMO or at most the LUMO+1 are occupied by the electrons transferred from the Ca atoms. So the reduced intensity of the first feature reveals that the final states are mainly composed of the LUMO and LUMO+1 states. This conclusion is the premise of studying the molecular orientation.

In the XAS measurement, the absorption cross section

of a K-shell (here C 1s) resonance depends on the projection of the x-ray electric field vector onto the final state orbital involved in the transition. The absorption intensity of a C 1s$\rightarrow \pi^*$ transition is the maximum/zero if the electric field vector is parallel/perpendicular to the π^* orbital. The main chain of ITIC is planar (Fig. 1(a)); the LUMO and LUMO + 1 are π^* nature according to our DFT calculations. So the molecular orientation in the ITIC film can be deduced from the angle-dependent XAS spectra. In Fig. 3 θ refers to the angle between the incoming x-ray beam and the sample surface as indicated by the inset in Fig. 3(b). The first feature at 284.4 (or 284.3) eV mainly corresponds to the C 1s$\rightarrow$LUMO (probably also LUMO + 1) transition as discussed previously. The intensity of this feature changes remarkably with angle. So the ITIC molecules in the film have a significant preferable orientation. More specifically, the intensity of the first feature decreases monotonically with the angle increasing from 15° to 90°. Considering the fact that the LUMO and LUMO + 1 orbitals (π^*) are perpendicular to the plane of the main chain of ITIC, the molecules predominantly adopt the face-on orientation on all the three substrates.

The substrates used in this work and in actual OSC fabrication are all inert, and thus the interfacial chemical interaction is negligible. What determines the molecular orientation should be the intrinsic inter-molecular interaction and the substrate morphology. The Si:H (111) substrate is atomically smooth. The naturally oxidized Al (111) substrate is nearly atomically smooth. The ITO substrate has the surface roughness of several nm (revealed by atomic force microscopy images not shown here), but the ITIC molecules still predominantly have a face-on orientation. Therefore, we think that ITIC molecules prefer to form face-on oriented film on inert substrates as long as the surfaces of the substrates are not too rough. The different degrees of the face-on orientation on some other substrates reported in Refs. [13], [14], and [28] should be due to the different surface roughness of the substrates. The highly disordered orientation for the ITIC film on the PEDOT:PSS covered Si wafer[27] is most probable due to the very rough and mutual penetrating ITIC/PEDOT:PSS interface (the surface layers of the PEDOT:PSS film are redissolved when spin-coating ITIC).

4. Conclusions

The $E_{\mathrm{ict}-}$ of ITIC is 4.00 ± 0.05 eV and close to that of $PC_{61}BM$, which provides a reference not only for selecting matching donor materials in fabricating OSCs but also for modifying the molecular structure of ITIC to obtain more advanced acceptor materials. The ITIC molecules prefer to form face-on oriented film as long as the substrate surface is not too rough. So one can control the charge transporting property of ITIC-based devices by fabricating ITIC/donor and ITIC/electrode interfaces with the appropriate morphology.

References

[1] Yu G, Gao J, Hummelen J C, Wudl F and Heeger A J 1995 *Science* **270** 1789

[2] Wienk M M, Kroon J M, Verhees W J, Knol J, Hummelen J C, van Hal P A and Janssen R A 2003 *Angew. Chem. Int. Ed.* **42** 3371

[3] Lin Y, Wang J, Zhang Z G, Bai H, Li Y, Zhu D and Zhan X 2015 *Adv. Mater.* **27** 1170

[4] Zhao W, Qian D, Zhang S, Li S, Inganäs O, Gao F and Hou J 2016 *Adv. Mater.* **28** 4734

[5] Li S, Ye L, Zhao W, Zhang, S, Mukherjee S, Ade H and Hou J 2016 *Adv. Mater.* **28** 9423

[6] Yang Y, Zhang Z G, Bin H, Chen S, Gao L, Xue L, Yang C and Li Y 2016 *J. Am. Chem. Soc.* **138** 15011

[7] Zhao W, Li S, Yao H, Zhang S, Zhang Y, Yang B and Hou J 2017 *J. Am. Chem. Soc.* **139** 7148

[8] Zhao F, Dai S, Wu Y, Zhang Q, Wang J, Jiang L, Ling Q, Wei Z, Ma W, You W, Wang C and Zhan X 2017 *Adv. Mater.* **29** 1700144

[9] Zhu J, Li S, Liu X, Yao H, Wang F, Zhang S, Sun M and Hou J 2017 *J. Mater. Chem. A* **5** 15175

[10] Yao H, Ye L, Hou J, Jang B, Han G, Cui Y, Su G M, Wang C, Gao B, Yu R, Zhang H, Yi Y, Woo H Y, Ade H and Hou J 2017 *Adv. Mater.* **29** 1700254

[11] Fei Z, Eisner F D, Jiao X, Azzouzi M, Röhr J A, Han Y, Shahid M, Chesman A S R, Easton C D, McNeill C R, Anthopoulos T D, Nelson J and Heeney M 2018 *Adv. Mater.* **30** 1705209

[12] Bao X, Zhang Y, Wang J, Zhu D, Yang C, Li Y, Yang C, Xu J and Yang R 2017 *Chem. Mater.* **29** 6766

[13] Hadmojo W T, Wibowo F T A, Ryu D Y, Jung I H and Jang S Y 2017 *ACS Appl. Mater. Interfaces* **9** 32939

[14] Park S H, Park, G E, Choi S, Park S Y, Park C G, Cho M J and Choi D H 2018 *Org. Electron.* **53** 151

[15] Wen S, Chen W, Huang G, Shen W, Liu H, Duan L, Zhang J and Yang R 2018 *J. Mater. Chem. C* **6** 1753

[16] Zhang Z, Liu W, Rehman T, Ju H X, Mai J, Lu X, Shi M, Zhu J, Li C Z and Chen H 2017 *J. Mater. Chem. A* **5** 9649

[17] Du Y Y, Chen G H, Li W J, Bai X Y, Lin D Q, Ju H, Hu S, Xu Q, Wang Y, Li X, Zhu J and Li H N 2018 *AIP Adv.* **8** 035015

[18] Tengstedt C, Osikowicz W, Salaneck W R, Parker I D, Hsu C H and Fahlman M 2006 *Appl. Phys. Lett.* **88** 053502

[19] Braun S, Salaneck W R and Fahlman M 2009 *Adv. Mater.* **21** 1450

[20] Lange I, Blakesley J C, Frisch J, Vollmer A, Koch N and Neher D 2011 *Phys. Rev. Lett.* **106** 216402

[21] Bao Q, Fabiano S, Andersson M, Braun S, Sun Z, Crispin X, Berggren M, Liu X and Fahlman M 2016 *Adv. Funct. Mater.* **26** 1077

[22] Xu Z, Chen L M, Chen M H, Li G and Yang Y 2009 *Appl. Phys. Lett.* **95** 013301

[23] Sehati P, Braun S, Lindell L, Liu X, Andersson L M and Fahlman M 2010 *IEEE J. Sel. Top. Quantum Electron.* **16** 1718

[24] Schuettfort T, Thomsen L and McNeill C R 2013 *J. Am. Chem. Soc.* **135** 1092

[25] Sun, K, Xiao Z, Lu S, Zajaczkowski W, Pisula W, Hanssen E, White J M, Williamson R M, Subbiah J, Ouyang J, Holmes A B, Wong W W and Jones D J 2015 *Nat. Commun.* **6** 6013

[26] Li S, Liu W, Li C Z, Shi M and Chen H 2017 *Small* **13** 1701120

[27] Shi X, Zuo L, Jo S B, Gao K, Lin F, Liu F and Jen A K Y 2017 *Chem. Mater.* **29** 8369

[28] Zheng Y, Huang J, Wang G, Kong J, Huang D, Mohadjer Beromi M, Hazari N, Taylor A D and Yu J 2018 *Mater. Today* **21** 79

[29] Chen G H, Bai X Y, Li W J, Du Y Y, Lin D Q, Li H Y, Wang J O, Qian H J, Wu R, Ibrahim K and Li H N 2017 *J. Phys. Chem. C* **121** 19097

[30] Sheng C Q, Wang P, Shen Y, Li Y J, Zhang W H, Xu F Q, Zhu J F, Lai G Q and Li H N 2012 *Chin. Phys. B* **21** 017102

[31] Li H N, Yang H, Wang X X, Ni J F, Wang P, Meng L, Wang X B, Kurash I, Qian H J, Wang J O and Liu Z Y 2009 *J. Phys.: Condens. Matter* **21** 265502

[32] Davids P S, Saxena A and Smith D L 1995 *J. Appl. Phys.* **78** 4244

[33] Oehzelt M, Koch N and Heimel G 2014 *Nat. Commun.* **5** 4174

[34] Omer B M 2015 *Chin. Phys. Lett.* **32** 088801